





Sven Kochmann 
An T. H. Le 
Ryan Hill 
Sergey N. Krylov 

Department of Chemistry and
Centre for Research on
Biomolecular Interactions, York
University, Toronto, Ontario,
Canada

Received June 30, 2018

Revised July 25, 2018

Accepted July 26, 2018

Research Article

Predicting efficiency of NECEEM-based partitioning of protein binders from nonbinders in DNA-encoded libraries

Nonequilibrium capillary electrophoresis of equilibrium mixtures (NECEEM) is an affinity method for separating binder-target complexes from nonbinders by gel-free CE. NECEEM is a promising high-efficiency method for partitioning protein binders from nonbinders in DNA-encoded libraries (DEL), such binders are used as “hits” in drug development. It is important to be able to predict the efficiency of NECEEM-based partitioning, which is the efficiency of collecting binders while removing nonbinders for a specific protein and a specific DEL with a minimum of empirical information. Here, we derive and study the dependence of efficiency of NECEEM-based partitioning on electrophoretic mobilities of the protein and the DNA moiety in DEL compounds. Our derivation is based upon a previously found relation between the electrophoretic mobility of protein-binder complex and measured electrophoretic mobilities of the protein and unbound DEL and their estimated sizes. The derivation utilizes the assumption of Gaussian shapes of electrophoretic peaks and the approximation of the efficiency of partitioning by the background of nonbinders – a fraction of nonbinders, which elutes along with protein-binder complexes. Our results will serve as a guiding tool for planning the NECEEM-based partitioning of protein binders from non-binders in DELs. In particular, it can be used to estimate a minimum number of rounds of partitioning required for the desired level of DEL enrichment.

Keywords:

DNA-encoded libraries / Efficiency of partitioning / Nonequilibrium capillary electrophoresis of equilibrium mixtures / Protein binders

DOI 10.1002/elps.201800270



Additional supporting information may be found online in the Supporting Information section at the end of the article.

1 Introduction

Most therapeutic targets are proteins and most modern drugs are protein binders, i.e. compounds capable of forming stable noncovalent complexes with their protein targets [1, 2]. A major approach to find protein binders is the screening of large combinatorial libraries of small molecules such as DNA-encoded libraries (DELs) with as many as 10^{10} different compounds each possessing a DNA-tag encoding its

structure (see Ref. [3] for a comprehensive review on DELs including their preparation) [3–7]. Screening DELs for protein binders includes four major steps (Fig. 1A) [8–12]. The first step is multiple consecutive rounds of affinity partitioning of binders from nonbinders; this step results in a binder-enriched DEL. The second step is sequencing DNA tags on the compounds in the binder-enriched DEL and decoding the small-molecule structures based on the sequence information. The third step is synthesis of individual DNA-free compounds. The final step is confirmation of binding of individual DNA-free compounds to the target protein and measurements of binding parameters such as the equilibrium constant, K_d , and the rate constant, k_{off} , of dissociation of protein-binder complex.

The first step, i.e. the partitioning of binders (B) from nonbinders (N), is the most critical step in DEL screening [5, 13]. Partitioning is schematically depicted in Fig. 1B,

Correspondence: Dr. Sergey N. Krylov, Department of Chemistry and Centre for Research on Biomolecular Interactions, York University, Toronto, Ontario M3J 1P3, Canada

Fax: +1 416 736 5936

E-mail: skrylov@yorku.ca

Abbreviations: **CAII**, carbonic anhydrase II; **DEL**, DNA-encoded library; **NECEEM**, nonequilibrium capillary electrophoresis of equilibrium mixtures; **SA**, streptavidin

Color Online: See the article online to view Figs. 1–3 in color.

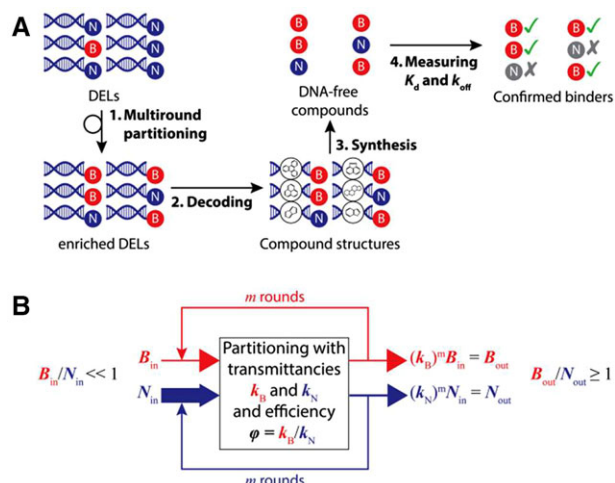


Figure 1. A: Schematic representation of the four major steps in DEL screening for protein binders. B: Schematic representation of the features of the step of partitioning of binders (B) from non-binders (N). B_{in} and N_{in} are amounts of binders and non-binders at the input of partitioning, respectively. B_{out} and N_{out} are amounts of binders and nonbinders at the input of partitioning, respectively. Each round of partitioning is performed with transmittancies k_B and k_N of binders and nonbinders, respectively. m is the number of rounds.

where B_{in} , N_{in} , and B_{out} , N_{out} are amounts of binders and non-binders at the input and output of partitioning (see Ref. [14] for evaluation of B_{in} , N_{in} , B_{out} , and N_{out}), and m is the number of consecutive partitioning rounds. Any partitioning method acts as a filter letting binders pass while cutting off non-binders; we adopted the term *transmittance* from optical filters to describe this filter function. Transmittancies of a single round ($m = 1$) of partitioning for binders and non-binders can be defined as $k_B = B_{out} / B_{in}$ and $k_N = N_{out} / N_{in}$, respectively. The single-round efficiency of partitioning of binders from nonbinders can then be defined as $\varphi = k_B / k_N$. In ideal partitioning, $k_B = 1$, $k_N = 0$, and $\varphi \rightarrow \infty$. In real partitioning, the value of $k_B \approx 1$ can be achieved so that $\varphi \approx 1/k_N$ [15]. Maximizing φ requires minimizing k_N , which is an absolute measure of the background after partitioning caused by nonbinders – a smaller value of k_N corresponds to a lower background. There is a continuing effort to develop partitioning methods with low background or small values of k_N [16–19]. A partitioning method can be considered highly efficient if its background is of the order of magnitude of binder abundance in the starting DEL (B_{in} / N_{in}), which can be as low as 10^{-5} [20]. Highly-efficient partitioning with such abundance can uniquely facilitate DEL enrichment to the level of $B_{out} / N_{out} \approx 1$ in just a single round; therefore, we consider 10^{-5} as a maximum acceptable value for k_N .

We suggested nonequilibrium capillary electrophoresis of equilibrium mixtures (NECEEM) as an efficient tool for partitioning protein binders from nonbinders in DELs [21]. NECEEM is an affinity method for separating binder-target

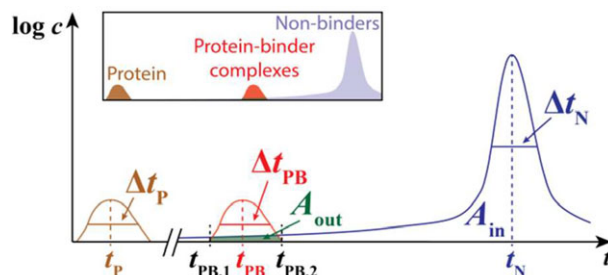


Figure 2. Schematic electropherogram of NECEEM-based partitioning of binders from nonbinders showing the peaks of protein, protein-binder complexes, and nonbinders (the unbound DEL compounds). The peaks are assumed to have Gaussian shapes. The transmittance k_N and, thus, the background after partitioning is simply the ratio between the green area and the total area under the peak of nonbinders (Eq. (5)). Note that the concentration axis is in log scale and the presented case corresponds to $k_N \approx 10^{-5}$.

complexes from nonbinders by gel-free CE. NECEEM was developed by us and proven by others to be an efficient tool for aptamer selection [20, 22–24]; in aptamer selection, values of $k_N \approx 10^{-5}$ for one-round selection were demonstrated with lower values being potentially achievable [20]. In principle, these values should also be achievable for binder selection from DELs. In NECEEM-based partitioning, the protein-binder complexes migrate faster and exit the capillary before nonbinders, which excludes the contribution of non-binder adsorption onto the capillary wall to the background. Therefore, the background in NECEEM-based partitioning is caused solely by the overlapping between the electrophoretic peak of protein-binder complexes and that of nonbinders (Fig. 2). This deterministic nature of the background of non-binders in NECEEM makes it possible to predict its lowest theoretically-achievable level if the shapes and positions of these two peaks are defined. Accordingly, the goal of this study was (i) to develop an approach for such prediction and (ii) proof the theoretical feasibility of NECEEM for one-round binder selection from DELs by achieving a maximum background of $k_N \approx 10^{-5}$.

The efficiency of partitioning increases with increasing separation resolution of the peaks of protein-binder complexes and nonbinders. The resolution as a measure of overlapping, in turn, depends on the sizes and charges of the protein and the DNA moiety of DEL compounds. Accordingly, we derived and studied the dependency of k_N on the sizes and charges of the protein and the DNA moiety in DEL compounds. We applied these dependencies to find the smallest protein size for which a desirable value $k_N \approx 10^{-5}$ can be theoretically achieved for a DEL with known published structures of DNA moieties [25]. The result of our study is a guiding tool for planning the NECEEM-based partitioning of protein binders from nonbinders in DELs.

2 Results and discussion

2.1 Peak parameters in an electropherogram

Electrophoretic peaks of unbound protein and unbound DEL (nonbinders) can be easily recorded as an electropherogram: intensity (proportional to analyte concentration) versus migration time, t (Fig. 2). The electropherogram provides positions of peak maxima and peak dispersions (full width at half maximum, FWHM) for the protein, t_P and Δt_P , and nonbinders, t_N and Δt_N , respectively. The values of t_P and t_N can be used to find electrophoretic mobilities of the protein, μ_P , and nonbinders, μ_N :

$$\begin{aligned}\mu_P &= \frac{l}{E} \frac{t_{\text{EOF}} - t_P}{t_{\text{EOF}} t_P} \\ \mu_N &= \frac{l}{E} \frac{t_{\text{EOF}} - t_N}{t_{\text{EOF}} t_N}\end{aligned}\quad (1)$$

Here t_{EOF} is the migration time of a neutral marker in the electropherogram; the neutral marker is propagated by the electro-osmotic flow (EOF) only. E is the strength of electric field and l is the distance from the position of start of electrophoresis to the point of detection.

2.2 Mobility of protein-binder complex

The found mobilities μ_P and μ_N allow predicting the electrophoretic mobility of the protein-binder complex (PB) [21]:

$$\mu_{\text{PB}} = \frac{d_P^2 \mu_P + (d_{\text{dsDNA}} L_{\text{dsDNA}} + d_{\text{ssDNA}} L_{\text{ssDNA}}) \mu_N}{d_P^2 + d_{\text{dsDNA}} L_{\text{dsDNA}} + d_{\text{ssDNA}} L_{\text{ssDNA}}}, \quad (2)$$

where d_P is the hydrodynamic size of the protein assumed to be globular, d_{dsDNA} and d_{ssDNA} are diameters of the single- and double-stranded regions, respectively, in the DNA moiety of DEL compounds, and L_{dsDNA} and L_{ssDNA} are lengths of these regions (for details on these parameters see Fig. 3 in [21]). Equation (2) was tested on a series of DNA moieties (several DNA chimeras and a DNA moiety used in actual DELs) and two proteins (streptavidin (SA) and carbonic anhydrase II (CAII)) and showed to predict mobility deviating from the experimental one by less than 11% [21].

The value of d_P can be found from structural data or accurately estimated from a known diffusion coefficient of the protein, D_P , using the Stokes-Einstein equation [26]

$$d_P = \frac{RT}{3\pi\eta D_P N_A} 10^9 \text{ [nm]}, \quad (3)$$

where $R \approx 8.31 \text{ kg m}^2 \text{ s}^{-2} \text{ K}^{-1} \text{ mol}^{-1}$ is the gas constant, T is the absolute temperature in K, η is the solvent viscosity, and $N_A \approx 6.02 \times 10^{23} \text{ mol}^{-1}$ is the Avogadro number. For example, we can estimate for SA ($D_P \approx 9 \times 10^{-11} \text{ m}^2 \text{ s}^{-1}$) [27] at $T \approx 300 \text{ K}$ and in water ($\eta \approx 9.0 \times 10^{-4} \text{ kg m}^{-1} \text{ s}^{-1}$) that $d_P = 5.4 \text{ nm}$ which is in good agreement with 5.3 nm found in crystallographic studies [28]. Under the same conditions and for CAII ($D_P \approx 1 \times 10^{-10} \text{ m}^2 \text{ s}^{-1}$) [29], Eq. (3) leads to

$d_P = 4.4 \text{ nm}$, which is also in good agreement with 4.5 nm found in crystallographic studies [30].

For the DNA moiety, the diameters are $d_{\text{dsDNA}} = 2.6 \text{ nm}$ and $d_{\text{ssDNA}} = 1.6 \text{ nm}$, which include the hydration shells around the dsDNA and ssDNA regions [31]. The lengths of moieties can be calculated by $L_{\text{dsDNA}} = b_{\text{dsDNA}} \times n_{\text{dsDNA}}$, $L_{\text{ssDNA}} = b_{\text{ssDNA}} \times n_{\text{ssDNA}}$, where $b_{\text{dsDNA}} = 0.34 \text{ nm}$ and $b_{\text{ssDNA}} = 0.43 \text{ nm}$ are the lengths of dsDNA and ssDNA monomers and n_{dsDNA} and n_{ssDNA} are numbers of nucleotides in all double-stranded regions and all single-stranded regions, respectively [32].

The predicted value of μ_{PB} can be used to predict the migration time of the complex:

$$t_{\text{PB}} = t_{\text{EOF}} \frac{l}{\mu_{\text{PB}} E t_{\text{EOF}} + l} \quad (4)$$

Based on the observed behavior, we assume the dispersion of the peak of complexes, Δt_{PB} to be equal to the dispersion of nonbinders, $\Delta t_{\text{PB}} \approx \Delta t_N$, which is always larger than that of the protein because of the heterogeneity of DELs. The values of t_{PB} and Δt_{PB} define the binder-collection window which is necessary for defining and predicting the background of nonbinders in NECEEM-based partitioning (Fig. 2).

2.3 Defining k_N for its prediction

k_N is defined as the ratio between the number of nonbinders remaining after partitioning, N_{out} , and the number of nonbinders at the input of partitioning, N_{in} , i.e. $k_N = N_{\text{out}}/N_{\text{in}}$. In an electropherogram (Fig. 2), N_{out} and N_{in} correspond, respectively, to the area of the background (A_{out}) and the total area of the peak of nonbinders (A_{in}). Therefore, assuming that all the peaks have a Gaussian shape, k_N can be calculated as

$$\begin{aligned}k_N &= \frac{N_{\text{out}}}{N_{\text{in}}} = \frac{A_{\text{out}}}{A_{\text{in}}} = \frac{\int_{t_{\text{PB},1}}^{t_{\text{PB},2}} I_{N,\text{max}} \exp\left(\frac{-(t - t_N)^2}{2\sigma_N^2}\right)}{\int_{-\infty}^{+\infty} I_{N,\text{max}} \exp\left(\frac{-(t - t_N)^2}{2\sigma_N^2}\right)} \\ &= \frac{\int_{t_{\text{PB},1}}^{t_{\text{PB},2}} \exp\left(\frac{-(t - t_N)^2}{2\sigma_N^2}\right)}{\int_{-\infty}^{+\infty} \exp\left(\frac{-(t - t_N)^2}{2\sigma_N^2}\right)}\end{aligned}\quad (5)$$

where $\sigma_N = 0.425 \times \Delta t_N$. The limits of integration in the upper integral are defined as $t_{\text{PB},1} = t_{\text{PB}} - 3\sigma_{\text{PB}}$ and $t_{\text{PB},2} = t_{\text{PB}} + 3\sigma_{\text{PB}}$, respectively, to capture 99.73% of the peak. Taking into consideration our assumption of $\Delta t_{\text{PB}} \approx \Delta t_N$, we can rewrite these limits as $t_{\text{PB},1} = t_{\text{PB}} - 3\sigma_N = t_{\text{PB}} - 1.275 \times \Delta t_N$ and $t_{\text{PB},2} = t_{\text{PB}} + 3\sigma_N = t_{\text{PB}} + 1.275 \times \Delta t_N$.

The definite integral with infinite limits in the denominator of Eq. (5) can be simply written as

$$\int_{-\infty}^{+\infty} \exp\left(\frac{-(t - t_N)^2}{2\sigma_N^2}\right) \approx \Delta t_N \quad (6)$$

In contrast, the indefinite integral function of a Gauss function is the non-elementary error-function, which cannot be evaluated in closed form [33, 34]. Thus, the integral with non-infinite limits in the numerator must be found numerically or by approximation.

2.4 Numerical study of k_N

For our further study we used the following equation obtained from Eqs. (5) and (6):

$$k_N = \frac{\int_{t_{PB} - 1.275\Delta t_N}^{t_{PB} + 1.275\Delta t_N} \exp\left(\frac{-(t - t_N)^2}{0.36\Delta t_N^2}\right) dt}{\Delta t_N} \quad (7)$$

As example, we evaluated some of the models described in Ref. 25 for both SA and CAII proteins and a series of different DNA moieties used in actual DELs (see Supporting information Table 1 in ESI). The original electropherograms of this reference (see Supporting information Figs. 1 and 2 in ESI) were used to determine t_P , t_N , Δt_N , and t_{EOF} . The value of μ_{PB} was calculated using Eq. (2) (see details above). The value of t_{PB} was calculated with Eq. (4). The value of Δt_{PB} was assumed to be equal to Δt_N as justified above. The theoretically achievable values of k_N were then calculated with Eq. (7). All obtained data is available in the Supporting information Figs. 1, 2 and Table 2.

We found that for large proteins such as SA (53 kDa) and CAII (29 kDa) and DNA moieties of 40–117 bases the theoretically achievable values of k_N are $<10^{-20}$, which is several orders of magnitudes lower than the desired maximum value of 10^{-5} . The lowest k_N values are achieved for 1:1 (P:B) complexes (from $<10^{-300}$ up to 10^{-144}) while the highest value of 10^{-20} is for a 1:4 complex for SA and a biotin ligand with a large DNA moiety (117 bases). The results for different P:B ratios show that k_N raises by 20–40 orders of magnitude with each step of increasing binding stoichiometry, i.e. when another biotin DNA ligand binds to a biotin-SA complex (up to a ratio of 1:4). This extreme rise in k_N suggests that small and medium sized DNA moieties (40–117 bases) have a great influence on the mobility of the protein complex even for large proteins such as SA. In turn, such DNA moieties can significantly reduce the efficiency of NECEEM-based partitioning of binders from nonbinders in DELs.

2.5 Influence of protein size on k_N

The DNA moiety possesses a great electric charge because every nucleotide bears a single negative charge. Typically, proteins bear a much lower net charge. In our example system (pH 8, 50 mM TRIS·HCl) both SA and CAII possess the same charge to size ratio resulting in the same electrophoretic mobility of about $-4.3 \pm 0.2 \text{ mm}^2 (\text{kVs})^{-1}$. In contrast, the mobility of DNA moieties, independent of their length, possess a 6 × higher mobility ($-26.5 \pm 0.3 \text{ mm}^2 (\text{kVs})^{-1}$). Thus, in the first approximation, proteins can be considered

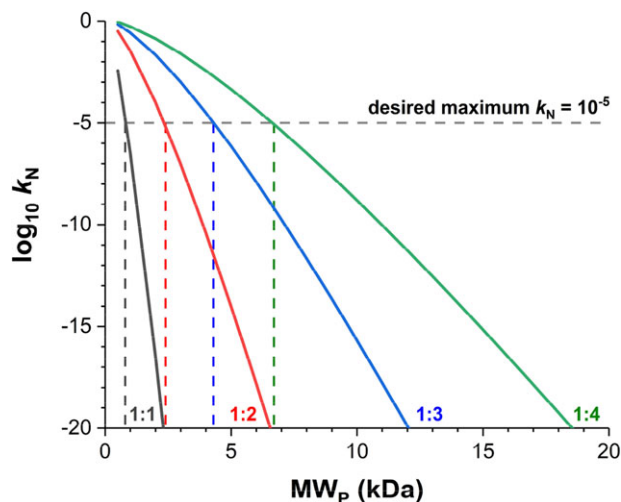


Figure 3. Transmittance of nonbinders, k_N , as a function of the molecular weight of the target protein, MW_p , for different binding stoichiometries and a typical DNA moiety present in a DEL (117 base pairs). The results indicate that in NECEEM-based partitioning, target proteins should have at least a molecular weight of 0.8, 2.4, 4.3, and 6.7 kDa for P:B ratios of 1:1, 1:2, 1:3, and 1:4, respectively.

electrical neutral ($\mu_p = 0$) in contrast to the DNA moiety. This assumption allows neglecting the first term in the numerator of Eq. (2). Further, the protein diameter d_p can be estimated by

$$d_p = 1.32 \times MW_p^{1/3} \text{ [nm]}, \quad (8)$$

where MW_p is the molecular weight of the protein in kDa [35]. Combining Eq. (8) with Eq. (2) and using the assumption that $\mu_p = 0$ gives:

$$\mu_{PB} = \frac{(d_{dsDNA} L_{dsDNA} + d_{ssDNA} L_{ssDNA}) \mu_N}{1.74 \times MW_p^{2/3} + d_{dsDNA} L_{dsDNA} + d_{ssDNA} L_{ssDNA}} \quad (9)$$

We used Eq. (9) to study the dependence of k_N on MW_p (which relates to the protein size) in a range of 1–20 kDa and a stoichiometry up to 1:4 (targets with small MW_p and high stoichiometry constitute a greater challenge for NECEEM-based partitioning of binders from nonbinders). The rest of parameters, which relate solely to DEL, were taken from Supporting Information Table 2. The results are listed in Supporting Information Table 3 and depicted in Fig. 3. We can see that the smallest protein size for which a desirable value $k_N \approx 10^{-5}$ can be theoretically achieved is 0.8 kDa, 2.4 kDa, 4.3 kDa, and 6.7 kDa for a complex binding stoichiometry of 1:1, 1:2, 1:3, and 1:4, respectively. This result suggests that NECEEM-based partitioning of binders may work for small oligopeptides and proteins but becomes inefficient for smaller peptides with molecular weights below the above-mentioned values. Note that the found values of k_N are theoretically achievable minima obtained for ideal Gaussian peaks. The real peak of nonbinders may have non-Gaussian fronting (because of the concentration, weak binders, etc.) which will make real k_N values larger than the estimates found here.

2.6 k_N of other partitioning methods

We were unable to find any data on background calculations or measurements for other partitioning methods, which makes it impossible to directly compare background in NECEEM-based partitioning with those of other partitioning methods. However, most partitioning methods are based on chromatography and filtration and require multiple-round selection because of their low efficiency of partitioning or high background [36, 37]. The need of multiple rounds strongly suggests that the values of k_N are far above 10^{-5} in these partitioning methods. In contrast, we show here that NECEEM is theoretically feasible of doing single-round selection with k_N far below 10^{-5} .

3 Concluding remarks

In this study, we developed an approach to predict the lowest theoretically achievable level of background (k_N) in NECEEM-based partitioning for selecting protein binders from DELs. The efficiency of partitioning increases with increasing separation resolution of the peaks of protein-binder complexes and nonbinders. The resolution, in turn, depends on the sizes and charges of the protein and the DNA moiety of DEL compounds. Accordingly, we derived and studied the dependency of k_N on the sizes and charges of the protein and the DNA moiety in DEL compounds. We found that the mobility of the protein is negligible in contrast to the mobility of the DNA moiety. Therefore, protein mobility can be considered zero, i.e. neutral charge. Furthermore, we found that the smallest protein sizes for which a desirable value of $k_N \approx 10^{-5}$ can be theoretically achieved are 0.8, 2.4, 4.3, and 6.7 kDa for a complex binding stoichiometries of 1:1, 1:2, 1:3, and 1:4, respectively. Our results will serve as a guiding tool for planning NECEEM-based partitioning of protein binders from nonbinders in DELs. In particular, they can be used to estimate a minimum number of rounds of partitioning required for the desired level of DEL enrichment.

This work was supported by the NSERC Canada (STPGP 463455). The authors thank Dr. Alexander Stasheuski for valuable discussions.

The authors have declared no conflict of interest.

4 References

- [1] Drews, J., *Science* 2000, 287, 1960–1964.
- [2] Santos, R., Ursu, O., Gaulton, A., Bento, A. P., Donadi, R. S., Bologa, C. G., Karlsson, A., Al-Lazikani, B., Hersey, A., Oprea, T. I., Overington, J. P., *Nat. Rev. Drug Discov.* 2016, 16, 19.
- [3] Goodnow, R. A. Jr., Dumelin, C. E., Keefe, A. D., *Nat. Rev. Drug Discov.* 2016, 16, 131.
- [4] Franzini, R. M., Randolph, C., *J. Med. Chem.* 2016, 59, 6629–6644.
- [5] Clark, M. A., Acharya, R. A., Arico-Muendel, C. C., Belyanskaya, S. L., Benjamin, D. R., Carlson, N. R., Centrella, P. A., Chiu, C. H., Creaser, S. P., Cuzzo, J. W., Davie, C. P., Ding, Y., Franklin, G. J., Franzen, K. D., Gefter, M. L., Hale, S. P., Hansen, N. J. V., Israel, D. I., Jiang, J., Kavarana, M. J., Kelley, M. S., Kollmann, C. S., Li, F., Lind, K., Mataruse, S., Medeiros, P. F., Messer, J. A., Myers, P., O'Keefe, H., Olliff, M. C., Rise, C. E., Satz, A. L., Skinner, S. R., Svendsen, J. L., Tang, L., van Vloten, K., Wagner, R. W., Yao, G., Zhao, B., Morgan, B. A., *Nat. Chem. Biol.* 2009, 5, 647.
- [6] Satz, A. L., *ACS Chem. Biol.* 2015, 10, 2237–2245.
- [7] Wichert, M., Krall, N., Decurtins, W., Franzini, R. M., Pretto, F., Schneider, P., Neri, D., Scheuermann, J., *Nat. Chem.* 2015, 7, 241–249.
- [8] Kleiner, R. E., Dumelin, C. E., Liu, D. R., *Chem. Soc. Rev.* 2011, 40, 5707–5717.
- [9] Neri, D., Lerner, R. A., *Annu. Rev. Biochem.* 2018, 87, 479–502.
- [10] Blakskjaer, P., Heitner, T., Hansen, N. J. V., *Curr. Opin. Chem. Biol.* 2015, 26, 62–71.
- [11] Ahn, S., Kahsai, A. W., Pani, B., Wang, Q.-T., Zhao, S., Wall, A. L., Strachan, R. T., Staus, D. P., Wingler, L. M., Sun, L. D., Sinnaeve, J., Choi, M., Cho, T., Wu, T. T., Hansen, G. M., Burnett, M. B., Lamerding, J. E., Bassoni, D. L., Gavino, B. J., Husemoen, G., Olsen, E. K., Franch, T., Costanzi, S., Chen, X., Lefkowitz, R. J., *Proc. Natl. Acad. Sci. U. S. A.* 2017.
- [12] Zimmermann, G., Li, Y., Rieder, U., Mattarella, M., Neri, D., Scheuermann, J., *ChemBioChem* 2017, 18, 853–857.
- [13] Hale, S. P., in: Goodnow, R. A. Jr. (Ed.), *A Handbook for DNA-Encoded Chemistry*, Wiley, 2014, p. 281–318.
- [14] Drabovich, A. P., Berezovski, M. V., Musheev, M. U., Krylov, S. N., *Anal. Chem.* 2009, 81, 490–494.
- [15] Drabovich, A. P., Berezovski, M., Okhonin, V., Krylov, S. N., *Anal. Chem.* 2006, 78, 3171–3178.
- [16] Wang, J., Gong, Q., Maheshwari, N., Eisenstein, M., Arcila, M. L., Kosik, K. S., Soh, H. T., *Angew. Chem. Int. Ed.* 2014, 53, 4796–4801.
- [17] Chan, A. I., McGregor, L. M., Jain, T., Liu, D. R., *J. Am. Chem. Soc.* 2017, 139, 10192–10195.
- [18] Wu, Z., Zhen, Z., Jiang, J.-H., Shen, G.-L., Yu, R.-Q., *J. Am. Chem. Soc.* 2009, 131, 12325–12332.
- [19] Shi, B., Zhou, Y., Huang, Y., Zhang, J., Li, X., *Bioorg. Med. Chem. Lett.* 2017, 27, 361–369.
- [20] Berezovski, M., Drabovich, A., Krylova, S. M., Musheev, M., Okhonin, V., Petrov, A., Krylov, S. N., *J. Am. Chem. Soc.* 2005, 127, 3165–3171.
- [21] Bao, J., Krylova, S. M., Cherney, L. T., Hale, R. L., Belyanskaya, S. L., Chiu, C. H., Shaginian, A., Arico-Muendel, C. C., Krylov, S. N., *Anal. Chem.* 2016, 88, 5498–5506.
- [22] Mendonsa, S. D., Bowser, M. T., *J. Am. Chem. Soc.* 2004, 126, 20–21.
- [23] Riley, K. R., Gagliano, J., Xiao, J., Libby, K., Saito, S., Yu, G., Cubicciotti, R., Macosko, J., Colyer, C. L., Guthold, M., Bonin, K., *Anal. Bioanal. Chem.* 2015, 407, 1527–1532.

- [24] Tok, J., Lai, J., Leung, T., Li Sam Fong, Y., *Electrophoresis* 2010, *31*, 2055–2062.
- [25] Bao, J., Krylova, S. M., Cherney, L. T., Hale, R. L., Belyanskaya, S. L., Chiu, C. H., Arico-Muendel, C. C., Krylov, S. N., *Anal. Chem.* 2015, *87*, 2474–2479.
- [26] Young, M. E., Carroad, P. A., Bell, R. L., *Biotechnol. Bioeng.* 2004, *22*, 947–955.
- [27] Banks, D. S., Tressler, C., Peters, R. D., Hofling, F., Fradin, C., *Soft Matter* 2016, *12*, 4190–4203.
- [28] Hendrickson, W. A., Pähler, A., Smith, J. L., Satow, Y., Merritt, E. A., Phizackerley, R. P., *Proc. Natl. Acad. Sci. USA* 1989, *86*, 2190–2194.
- [29] Okada, Y., Takeda, S., Tanaka, Y., Belmonte, J.-C. I., Hirokawa, N., *Cell* 2005, *121*, 633–644.
- [30] Eriksson, A. E., Jones, T. A., Liljas, A., *Proteins: Struct. Funct. Bioinf.* 2004, *4*, 274–282.
- [31] Schneider, B., Patel, K., Berman, H. M., *Biophys. J.* 1998, *75*, 2422–2434.
- [32] Meagher Robert, J., Won, J. I., McCormick Laurette, C., Nedelcu, S., Bertrand Martin, M., Bertram Jordan, L., Drouin, G., Barron Annelise, E., Slater Gary, W., *Electrophoresis* 2005, *26*, 331–350.
- [33] Abramowitz, M., Stegun, I. A., *Handbook of Mathematical Functions: With Formulas, Graphs, and Mathematical Tables*, Dover Publications, 1964.
- [34] Press, W. H., *Numerical Recipes 3rd Edition: The Art of Scientific Computing*, Cambridge University Press, 2007.
- [35] Erickson, H. P., *Biol. Proced. Online* 2009, *11*, 32.
- [36] Labrou, N. E., *J. Chromatogr. B: Biomed. Sci. Appl.* 2003, *790*, 67–78.
- [37] Woodbury, C. P., Von Hippel, P. H., *Biochemistry* 1983, *22*, 4730–4737.